

Phylogenetic relationships of a new catfish of the genus *Trichomycterus* (Siluriformes, Trichomycteridae) from the Brazilian Cerrado, and the role of Cenozoic events in the diversification of mountain catfishes

Wilson J. E. M. Costa¹, José Leonardo O. Mattos¹, Wagner M. S. Sampaio²,
Patrícia Giongo², Frederico B. de Almeida³, Axel M. Katz¹

1 *Laboratory of Systematics and Evolution of Teleost Fishes, Institute of Biology, Federal University of Rio de Janeiro, Caixa Postal 68049, CEP 21941-971, Rio de Janeiro, Brazil*

2 *Instituto de Pesquisa em Fauna Neotropical, Viçosa, MG, Brazil*

3 *Departamento de Medicina Veterinária, Universidade Federal de Viçosa, Viçosa, MG, Brazil*

<http://zoobank.org/F75C5C03-4C7E-4AF6-BD19-AF4182AFC24A>

Corresponding author: Wilson J. E. M. Costa (wcosta@acd.ufrj.br)

Academic editor: Nicolas Hubert ♦ Received 4 March 2022 ♦ Accepted 5 May 2022 ♦ Published 23 May 2022

Abstract

The Brazilian Cerrado highlands shelter the headwaters of the three largest South American hydrographic basins, where a great species diversity is concentrated, but some biological groups are still insufficiently known. The focal taxa of this study are trichomycterid catfishes of the subgenus *Cryptocambeva*, genus *Trichomycterus*, endemic to mountain areas of south-eastern Brazil. The primary objective of this study is to test through a molecular phylogeny if a new species collected in streams of the upper Rio Paraná basin draining the Serra da Canastra is sister to *T. macrotrichopterus*, endemic to the upper Rio São Francisco at another facet of the Serra da Canastra, as suggested by morphological data. The analysis corroborated sister group relationships between these two species, besides supporting four main clades in *Cryptocambeva*, each of them endemic to distinct mountain regions. A time-calibrated analysis supported the divergence timing between the new species and *T. macrotrichopterus* at the Pliocene, which is chronologically compatible with the final period of intense fluvial configuration re-arrangement, when São Francisco headwater streams were captured by the Paraná basin. The new species herein described is similar to *T. macrotrichopterus* and distinguished from all other species of *Cryptocambeva* by having a long pectoral-fin filament. These two species are distinguished from each other by characteristics of the latero-sensory system, colour pattern and bone morphology.

Key Words

molecular systematics, mountain biodiversity, osteology, paleo-drainages, Rio Paraná basin

Introduction

Studies on the Cerrado biota have quickly increased since the 1980s (Oliveira and Marquis 2002). However, some groups are still insufficiently known, including mountain catfishes of the Trichomycterinae (hereafter trichomycterines), the largest subfamily of the Neotropical siluriform family Trichomycteridae (Katz et al. 2018; Costa and Katz 2021). Trichomycterines occur in all areas of the Cerrado, but they are particularly diverse in mountain

ranges of south-eastern Brazil (Costa 1992; Triques and Vono 2004; Alencar and Costa 2006; Barbosa and Costa 2010; Costa and Katz 2021; Costa et al. 2021a, b).

The great trichomycterine species diversity concentrated in mountain ranges of south-eastern Brazil is probably a consequence of the past Cenozoic scenario, characterised by intense re-arrangements of the hydrographic systems due to generalised uplift during the Neogene (Riccomini et al. 2004; Valadão 2009). Events of drainage capture by neighbouring basins were frequent

until the Pliocene (Rezende et al. 2018), probably shaping the distribution pattern of fish species (Costa and Katz 2021; Costa et al. 2022a, b). Substantial evidence supports the upper and middle sections of the Rio Grande drainage, presently a main tributary of the upper Rio Paraná basin, as being formerly connected to the Rio São Francisco basin, a configuration that was changed after the capture of the Rio Grande drainage by the Rio Paraná basin during the Middle Miocene (Rezende et al. 2018).

The main focus of this study is an undescribed species of *Trichomycterus*, subgenus *Cryptocambeva* Costa, 2021, from the upper Rio Araguari drainage, upper Rio Paraná basin. *Cryptocambeva* comprises 16 species and is diagnosable by a unique morphology of the latero-posterior portion of the neurocranium and adjacent posterior region, including a relatively small posttemporo-supracleithrum separated by large interspaces from adjacent bones, and a narrow and long lateral extremity of the pterotic, with its tip extending beyond the lateral margin of the neurocranium (Costa 2021). The new taxon here described exhibits a long pectoral-fin filament, suggesting it is closely related to *T. macrotrichopterus* Barbosa & Costa, 2010, the only other species of *Cryptocambeva* having a similar long filament (Barbosa and Costa 2010). More interestingly, these two species were only found in rivers drainages separated by the Serra da Canastra, a mountain range of about 3,000 km² that is part of a series of mountain ranges situated between the upper Rio Paraná and upper Rio São Francisco basins. The northeastern facet of the Serra da Canastra is a major watershed divide between the headwaters of the Rio Araguari drainage, of the Rio Paranaíba drainage, upper Rio Paraná basin, where the new taxon was found, and the headwaters of the main course of the Rio São Francisco basin, where can be found the type locality of *T. macrotrichopterus* (Costa & Barbosa, 2010).

The primary objectives of this study are to perform a multigene phylogenetic analysis to test the phylogenetic positioning of the new taxon and to provide a formal description to it. The secondary objective is to conduct a dating analysis in order to establish if the estimated divergence timing for *Cryptocambeva* lineages from south-eastern Brazil is compatible with the available model for the temporal drainage network evolution.

Materials and methods

Specimens

Material used in this study included specimens previously deposited in ichthyological collections: Instituto de Biologia, Universidade Federal do Rio de Janeiro (UFRJ), and Museu de Zoologia, Universidade de São Paulo (MZUSP); and specimens collected in recent field studies using small dip nets (40 X 30 cm) and sieves (diameter 40–60 cm), and deposited in Centro de Ciências Agrárias e Ambientais, Universidade Federal do Maranhão (CICCAA). Collecting

permits were given by ICMBio (Instituto Chico Mendes de Conservação da Biodiversidade; permit numbers: 76588-1 and 38553-11) and IEF (Instituto Estadual de Florestas; permit number: 040/2020). Photographs of live specimens here presented were taken between about one-and-a-half hours and three hours after fish capture. Euthanasia followed methods approved by CEUA-CCS-UFRJ (Ethics Committee for Animal Use of Federal University of Rio de Janeiro; permit number: 065/18), using a buffered solution of tricaine methane sulphonate (MS-222) at a concentration of 250 mg/L, following AVMA (American Veterinary Medical Association) Guidelines (Leary et al. 2013) and the European Commission DGXI consensus for fish euthanasia (Close et al. 1996, 1997). Specimens were fixed in formalin for two weeks, and subsequently preserved in 70% ethanol, except specimens used in molecular analysis that were fixed in absolute ethanol. Comparative material is mainly deposited in UFRJ, but also includes specimens deposited in MZUSP, as well as in Museu de Ciências e Tecnologia, Pontifícia Universidade Católica, Porto Alegre (MCP), Muséum national d'Histoire Natural, Paris (MNHN), and Museu Nacional, Universidade Federal do Rio de Janeiro (MNRJ): *Trichomycterus brasiliensis* Lütken, 1874: MNHN 9575, 1 syntype (photograph); MNHN 18890303, 1 syntype (radiograph); UFRJ 4833, 5 ex.; UFRJ 4834, 3 ex. (C&S); UFRJ 4923, 2 ex.; UFRJ 4223, 2 ex.; Rio das Velhas basin, southeastern Brazil. *Trichomycterus brunoi* Barbosa & Costa, 2010: UFRJ 6030, holotype; UFRJ 5649, 11 paratypes; UFRJ 5658, 5 paratypes (C&S); UFRJ 5660, 2 paratypes; Rio Itabapoana basin, southeastern Brazil. *Trichomycterus candidus* (Miranda-Ribeiro, 1949): MNRJ 5209, holotype; MNRJ 11762, 14 paratypes; MNRJ 5356, 21 ex.; UFRJ 4926, 31 ex.; UFRJ 4928, 5 ex. (C&S); Rio Grande basin, southeastern Brazil. *Trichomycterus claudiae* Barbosa & Costa, 2010: UFRJ 6027, holotype; UFRJ 5684, 9 paratypes; UFRJ 5685, 3 paratypes (C&S); Rio Paraíba do Sul basin, southeastern Brazil. *Trichomycterus fuliginosus* Barbosa & Costa, 2010: UFRJ 6029, holotype; UFRJ 718, 5 paratypes; UFRJ 5207, 2 paratypes (C&S); UFRJ 3248, 1 paratype; MNRJ 18177, 7 (4 C&S) paratypes; Rio Paraíba do Sul basin, southeastern Brazil. *Trichomycterus giarettai* Barbosa & Katz, 2016: UFRJ 10109, holotype; UFRJ 9676, 8 paratypes; UFRJ 9739, 3 paratypes (C&S); Rio Paranaíba basin, central Brazil. *Trichomycterus macrotrichopterus* Barbosa & Costa, 2010: UFRJ 6031, holotype; UFRJ 5775, 3 paratypes; UFRJ 5776, 2 (C&S); UFRJ 8354, 1 ex.; upper Rio São Francisco basin, southeastern Brazil. *Trichomycterus mariamole* Barbosa & Costa, 2010: UFRJ 6026, holotype; UFRJ 5666, 17 paratypes; UFRJ 5142, 15 paratypes; UFRJ 5400, 3 paratypes (C&S); UFRJ 5401, 3 paratypes (C&S); UFRJ 5247, 15 paratypes; UFRJ 5688, 6 paratypes; UFRJ 7609, 4 ex.; UFRJ 7604, 6 ex.; UFRJ 1147, 2 ex.; Rio Paraíba do Sul basin, southeastern Brazil. *Trichomycterus mimonha* Costa, 1992: MZUSP 43343, holotype; MZUSP 43344, 7 paratypes; UFRJ 641, 7 paratypes; UFRJ 5209, 1 ex. (C&S); UFRJ 4731, 22 ex.; UFRJ 5665, 2 ex.; Rio Paraíba do Sul basin, southeastern Brazil. *Trichomycterus mirissumba* Costa, 1992: UFRJ

642,3 paratypes; UFRJ 4729,12 ex.; UFRJ 4730, 5 ex. (C&S); UFRJ 1300, 5 ex.; UFRJ 3391, 2 ex.; UFRJ 4729, 12 ex.; UFRJ 10486, 3 ex.; UFRJ 11843, 1 ex.; UFRJ 11656, 1 ex.; UFRJ 3864, 1 ex.; UFRJ 11677, 4; UFRJ 1638, 1 ex.; UFRJ 3366, 7 ex.; UFRJ 4100, 2 ex.; Rio Paraíba do Sul basin, southeastern Brazil. *Trichomycterus potschi* Barbosa & Costa, 2003: MCP 29061, holotype; UFRJ 4727, 11 paratypes; MCP 29062, 2 paratypes; UFRJ 4728, 5 paratypes (C&S); UFRJ 1636, 2 ex.; UFRJ 11002, 17 ex.; UFRJ 719, 10 ex.; Rio de Janeiro coastal river basins, southeastern Brazil. *Trichomycterus novalimensis* Barbosa & Costa, 2010: MZUSP 104536, holotype; MZUSP 37145, 15 paratypes; Rio das Velhas basin, southeastern Brazil. *Trichomycterus rubiginosus* Barbosa & Costa, 2010: MZUSP 104537, holotype; MZUSP 37168, 20 paratypes; Rio Paraopeba basin, southeastern Brazil. *Trichomycterus vermiculatus* (Eigenmann, 1917): FMNH 58077, holotype (x-rays); UFRJ 11787, 21 ex.; UFRJ 6095, 3 ex.; UFRJ 5462, 8 ex.; UFRJ 5465, 3 ex. (C&S); UFRJ 5463, 3 ex. (C&S); UFRJ 12564, 1 ex.; UFRJ 12563, 1 ex.; UFRJ 5464, 4 ex.; UFRJ 582, 12 ex.; UFRJ 7241, 2 ex.; UFRJ 3592, 16 ex.; UFRJ 571, 1 ex.; UFRJ 1143, 4 ex.; UFRJ 1131, 5 ex.; UFRJ 720, 3 ex.; Rio Paraíba do Sul basin, southeastern Brazil.

Morphological data

Measurements were made using landmarks proposed by Costa (1992) as modified by Costa et al. (2020a) and presented as percent of standard length (SL), or head length in measurements of head parts. Fin-ray counts and formulae were according to Bockmann and Sazima (2004), modified by Costa et al. (2020a), in which lower case Roman numerals indicate procurrent unsegmented unbranched rays of unpaired fins, upper case Roman numerals indicate segmented unbranched rays of any fin, and Arabic numerals indicate segmented branched rays of any fin. Vertebra counts included all free vertebrae, considering the compound caudal centrum as a single element. Taylor and Van Dyke's (1985) methodology was used to clear and stain specimens for osteological examination. Osteological terminology followed Costa (2021), and latero-sensory system terminology followed Arratia and Huaquin's (1995) pore nomenclature, modified by Bockmann and Sazima (2004). Illustrations of bones were made in a stereomicroscope Zeiss Stemi SV 6 with camera lucida. Bone landmark measurements were according to Costa and Katz (2021). Comparative material is listed in Costa (2021).

DNA extraction, amplification and sequencing

DNA was extracted from muscle tissues of the caudal peduncle, using DNeasy Blood & Tissue Kit (Qiagen), according to manufacturer's protocol. Amplification of DNA fragments was made using polymerase chain reaction

(PCR) method, with primers RAG2 TRICHO F and RAG2 TRICHO R (Costa et al. 2020b), and RAG2 MCF and RAG2 MCR (Cramer et al. 2011) for nuclear gene recombination activating 2 (RAG2); Cytb Siluri F and Cytb Siluri R (Villa-Verde et al. 2012) for the mitochondrial gene cytochrome b (CYTB); and ND4 H3 L11935 and H12857 (Palumbi et al. 1991) for the mitochondrial gene NADH dehydrogenase subunit 4 (ND4). Double-stranded PCR amplifications were made in 60 µl reactions with reagents at the following concentrations: 5× GreenGoTaq Reaction Buffer (Promega), 3.2 mM MgCl₂, 1 µM of each primer, 75 ng of total genomic DNA, 0.2 mM of each dNTP and 1 U of standard Taq polymerase or Promega GoTaq Hot Start polymerase. The thermocycling profile was: initial denaturation for 2–5 min at 94–95 °C; 35 cycles of denaturation for 0.5–1 min at 94–95 °C, annealing for 1–1.5 min at 45–52 °C and extension for 1–1.5 min at 72 °C; and terminal extension for 4–8 min at 72 °C. In all PCR reactions, negative controls without DNA were used to check contaminations. The PCR products were purified using the Wizard SV Gel and PCR Clean-Up System (Promega). Sequencing reactions were made using the BigDye Terminator Cycle Sequencing Mix (Applied Biosystems). Cycle sequencing reactions were performed in 20 µl reaction volumes containing 4 µl BigDye, 2 µl sequencing buffer 5× (Applied Biosystems), 2 µl of the amplified products (10–40 ng), 2 µl primer and 10 µl deionized water. The thermocycling profile was as follows: (1) 35 cycles of 10 s at 96 °C, 5 s at 54 °C and 4 min at 60 °C.

Phylogenetic analyses

The new species and twelve species representing all lineages of *Cryptocambeva* were included as terminal taxa in the analyses, besides four trichomycterine out-groups: *Trichomycterus albinotatus* Costa, 1992, a member of the subgenus *Humboldtglanis* Costa, 2021 that is sister to *Cryptocambeva* (Costa 2021); *Trichomycterus nigricans* Valenciennes, 1832, a distantly related species (Costa 2021); *Cambeva cf. cubataonis* (Bizerril, 1994), a member of the clade sister to *Trichomycterus s.s.* (Katz et al. 2018); and '*Trichomycterus areolatus* Valenciennes, 1846, a trichomycterine that is distantly related to *Trichomycterus s.s.* (Katz et al. 2018). GenBank accession numbers are provided in the Suppl. material 1: Tables S1, S2.

Alignment was conducted in Clustal W (Chenna et al. 2003) algorithm implemented in MEGAX (Kumar et al. 2018). No gap was found in alignments. The concatenated dataset was 2545 pb (1033 for CYTB, 693 for ND4, 819 for RAG2). This dataset was first analysed using a Maximum Likelihood (ML) approach in IQTREE 1.6.12 (Nguyen et al. 2015; Trifinopoulos et al. 2016), with partitions including each codon position for each gene, for which the best-fitting models as of molecular evolution, as described by Chernomor et al. (2016), were calculated using the Bayesian information criterion (BIC) of ModelFinder (Kalyaanamoorthy et al. 2017),

implemented in IQ-TREE. The list of partitions and their respective models of nucleotide substitution appear in the Suppl. material 1: Tables S1, S2. Three methods for assessing the reliability of internal branches were used in the ML analysis: the Shimodaira-Hasegawa-like procedure support (SH-aLRT; Guindon et al. 2010), the Bayesian-like transformation of SH-aLRT support (aBayes; Anisimova et al. 2011) and the ultrafast bootstrap support (UFBoot; Minh et al. 2013; Hoang et al. 2018), using 1000 replicates and default parameters as implemented in IQ-TREE.

The concatenated dataset was additionally analysed using Bayesian Inference (BI) with MrBayes 3.2.5 (Ronquist et al. 2012), using the best partition scheme and best-fit models of substitution (Suppl. material 1: Tables S1, S2) identified according to the Bayesian information criterion (BIC; Schwarz 1978) of PartitionFinder 2.1.1 (Lanfear et al. 2016), with the following parameters: two independent Markov chain Monte Carlo (MCMC) runs of two chains each for 30 million generations, with a tree sampling frequency of every 1000 generations. The convergence of the MCMC chains and the burn-in value

were assessed by evaluating the stationary phase of the chains using Tracer 1.7.1 (Rambaut et al. 2018). The BI final consensus tree and the Bayesian posterior probabilities were generated with the remaining tree samples after removing the first 25% samples as burn-in.

Divergence-time estimation

Terminal taxa were the same as above, but including additional outgroups: the trichomycterines *Scleronema minutum* (Boulenger, 1891) and *Ituglanis boitata* Ferrer, Donin & Malabarba, 2015; *Microcambeva ribeirae* Costa, Lima & Bizerril, 2004, a member of the Microcambevinae that is sister to the Trichomycterinae (Costa et al. 2020b); *Trichogenes longipinnis*, a basal trichomycterid (Katz et al. 2018); *Callichthys callichthys* (Linnaeus, 1758), a member of the loricarioid family Callichthyidae; *Nematogenys inermis* (Guichenot, 1848), the sister group to all other loricarioids (Betancur-R et al. 2015); and *Diplomystes nahuelbutaensis* Arratia, 1987, a basal member of the clade sister to the Loricarioidei (Sullivan et al. 2006; Betancur-R et al. 2015),

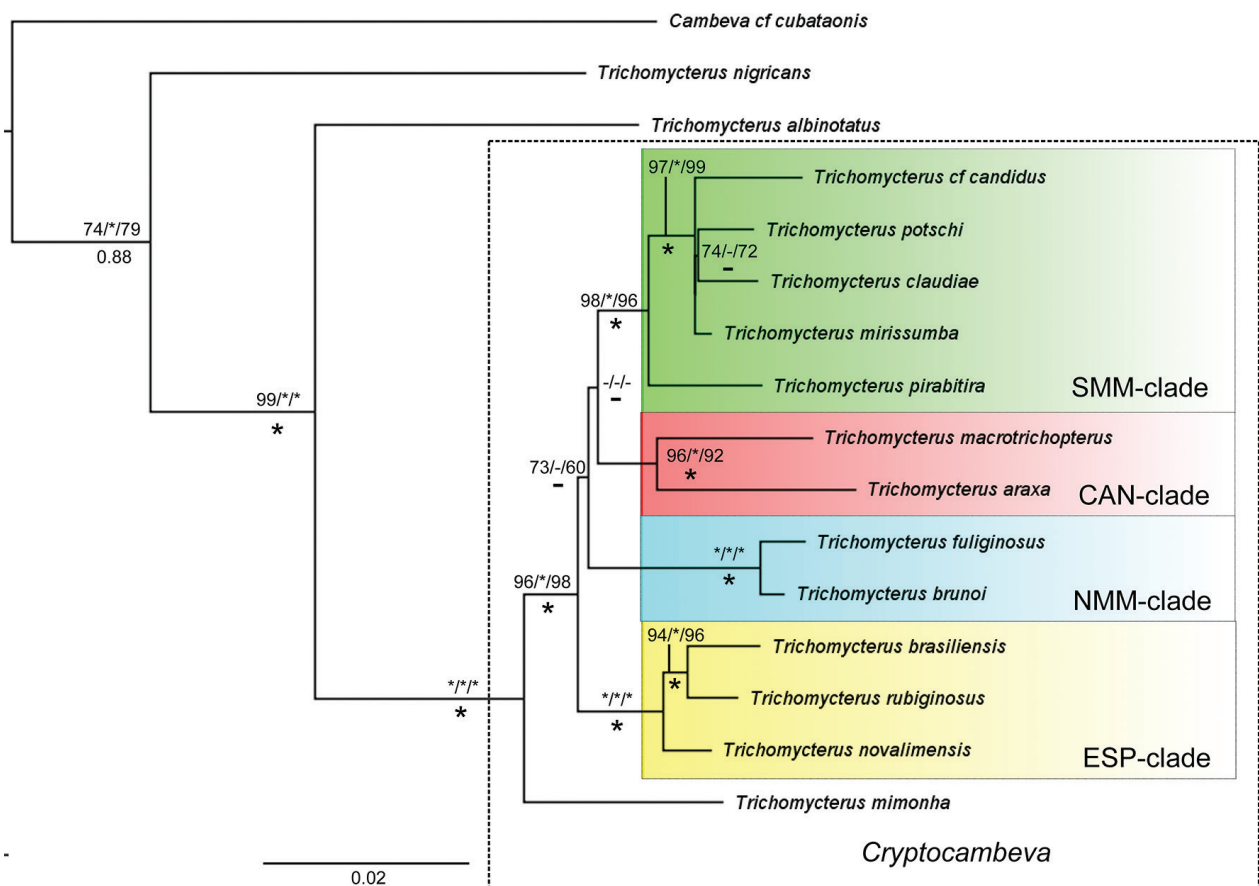


Figure 1. Phylogenetic tree generated by Maximum Likelihood analysis for 13 species of *Cryptocambeva* and four trichomycterine outgroups (most external out-group, '*Trichomycterus areolatus*', not depicted in the figure), using a multigene data set (CYTB, ND4 and RAG2, total of 2545 bp); numbers above branches are: SH-aLRT support (%) / aBayes support / ultrafast bootstrap support (%); numbers below branches are posterior probabilities from the Bayesian Inference; asterisks indicate maximum support values; minus sign indicate support values below 0.8 for aBayes support and posterior probability, and below 50% for SH-aLRT support and ultrafast bootstrap support. CAN-clade means Canastra clade; ESP-clade, Espinhaço clade; NMM-clade, northern Mantiqueira-Mar clade, and SMM-clade, southern Mantiqueira-Mar clade.

in which the analysis was rooted. DNA markers were the same as above; in addition, the best partition scheme and best-fit models were also calculated as above. The analysis was performed in BEAST v.1.10.4 (Suchard et al. 2018) using a relaxed molecular clock approach (uncorrelated relaxed molecular clock), and a Birth-Death process for the tree prior (Gernhard 2008). A single secondary calibration point was placed at the stem of the clade Trichomycteridae (normal prior distribution with mean age of 103.2 Mya, minimum age of 100.3 Mya, and standard deviation 1.5), an age estimated by Betancur-R et al. (2015). Two independent runs of Markov Chain Monte Carlo (MCMC), each runs with 50×10^6 generations were performed with sample frequency of 1000. The value of parameters of the analyses, convergence of the MCMC chains, effective sample size and the stationary distribution were evaluated using Tracer v. 1.7.1. Generated trees were combined in LogCombiner v.1.10.4 (Suchard et al. 2018) after applying a burn-in of the first 25% in each run. TreeAnnotator v.1.10.4 (Suchard et al. 2018) was used to obtain the maximum credibility tree and posterior probabilities.

Taxonomic accounts

Osteological structures included in the description are those that have informative variability to diagnose species of the eastern South American trichomycterine clade (e.g. Costa et

al. 2021c), comprising the mesethmoid and adjacent bones, jaw suspensorium and adjacent opercular bones, and the parurohyal. In the list of specimens, C&S means specimens cleared and stained for osteological examination. Geographical names are not tentatively translated to English, but follow Portuguese regional terms, making easier field identification and avoiding common errors when translating them.

Results

Phylogenetic analyses and divergence dating

The phylogenetic analyses generated identical trees, which corroborated the new taxon as sister to *T. macrotrichopterus* with high support values (Fig. 1). Like in previous analyses (e.g. Costa 2021), *Trichomycterus mimonha* Costa, 1992 appeared as sister to a clade containing all other species belonging to *Cryptocambeva*. This inclusive clade comprises four major well-supported clades that are geographically disjunct (Fig. 2): 1) the southern Mantiqueira-Mar clade (hereafter SMM-clade), comprising species endemic to river basins draining the southern Serra da Mantiqueira and the adjacent portion of the Serra do Mar; 2) the Canastra clade (hereafter CAN-clade), sister to the SMM-clade and comprising species endemic to the river basins draining the Serra da Canastra; 3) the northern

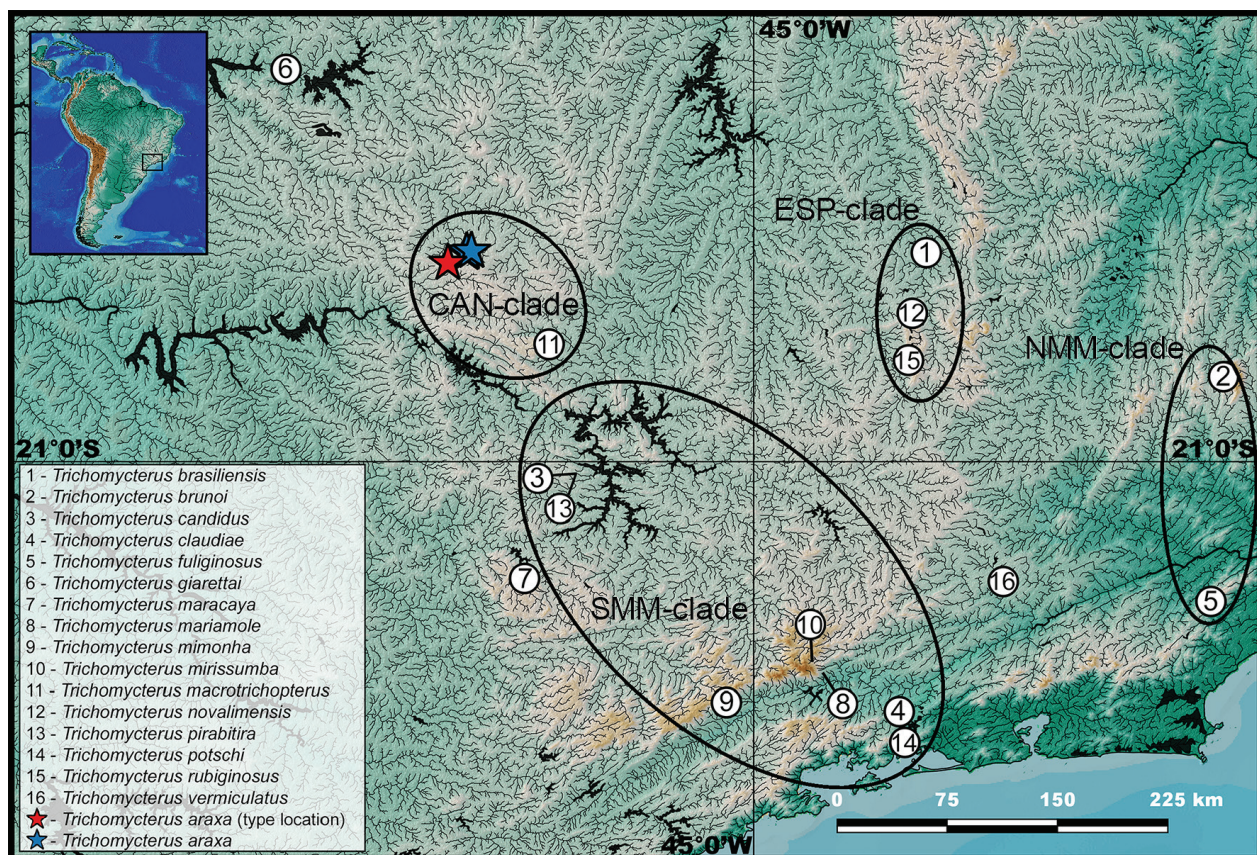


Figure 2. Geographical distribution of *Cryptocambeva*. CAN-clade means Canastra clade; ESP-clade, Espinhaço clade; NMM-clade, northern Mantiqueira-Mar clade, and SMM-clade, southern Mantiqueira-Mar clade.

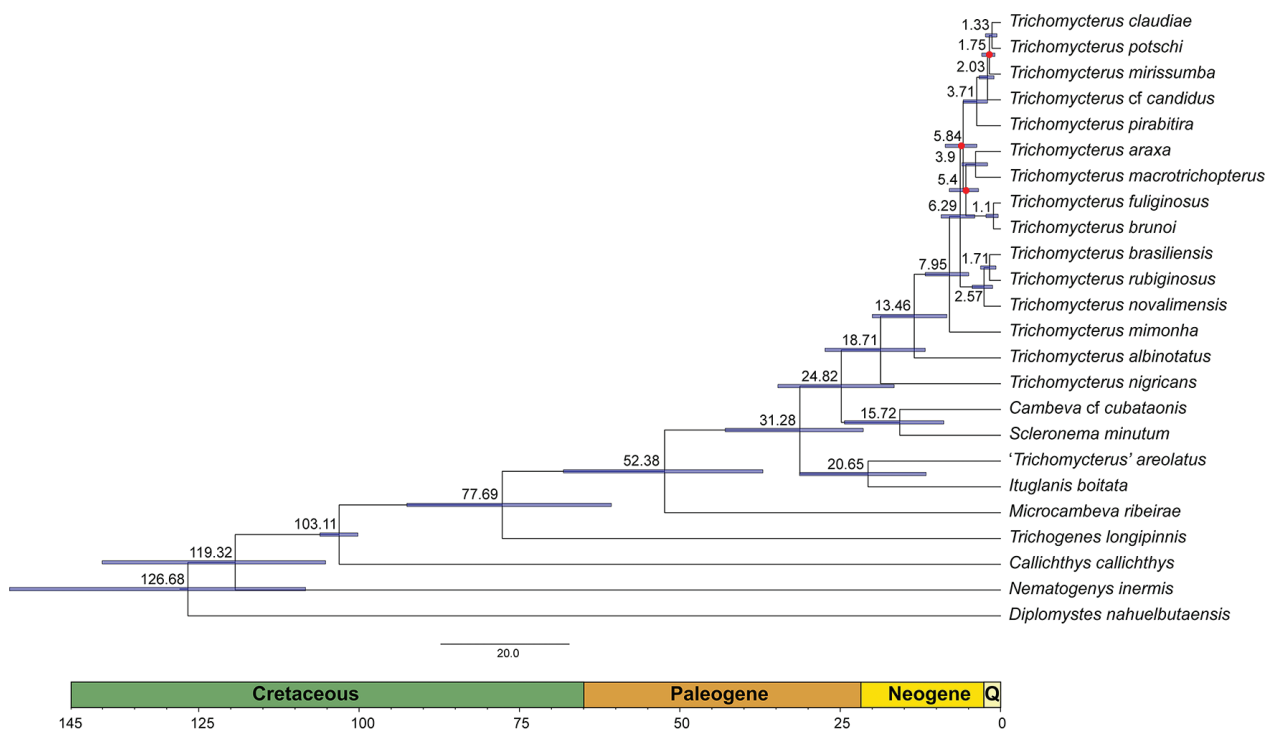


Figure 3. Time-scaled maximum credibility tree obtained from the Bayesian analysis in Beast for 13 species of *Cryptocambeva* and 11 outgroups, using a multigene data set (CYTB, ND4 and RAG2, total of 2545 bp). Numbers above the branches indicates the average age of the nodes and bars represent the 95% highest posterior densities intervals for the ages. Red dots indicate the nodes with posterior probabilities values inferior to 80. The time scale is express in millions of years.

Mantiqueira-Mar clade (hereafter NMM-clade), sister to the SMM-clade plus CAN-clade, and comprising species endemic to the river basins draining the northern Serra da Mantiqueira and the adjacent portion of the Serra do Mar; 4) and the Espinhaço clade (hereafter ESP-clade), sister to the SMM-clade plus CAN-clade plus NMM-clade, and comprising species endemic to the river basins draining the Serra do Espinhaço (Fig. 1). The time-calibrated analysis (Fig. 3) indicated an initial diversification of *Cryptocambeva*, with the splitting of *T. mimonha* and the clade containing the remaining species of the genus, during the Late Miocene, at about 8 Ma. According to the analysis, the divergence between the new species and *T. macrotrichopterus* occurred during the Pliocene, at about 4 Ma.

Taxonomical accounts

Trichomycterus araxa sp. nov.

<http://zoobank.org/367D112A-6969-4316-8456-D7AA9DE987AE>

Figs 4–7, 8A–C, Table 1

Holotype. UFRJ 7029, 53.6 mm SL; Brazil: Minas Gerais State: Araxá Municipality: stream tributary to Rio Capivara, a tributary of Rio Quebra Anzol, a tributary of the Rio Araguari subdrainage, Rio Paranaíba drainage, Rio Paraná basin, at Reserva Particular do Patrimônio Natural São Sebastião, 19°40'26"S, 47°02'24"W, about 970 m asl; A.M. Katz et al., 3 November 2021.

Paratypes. All from Brazil: Minas Gerais State: Araxá Municipality: Rio Araguari subdrainage, Rio Paranaíba drainage, Rio Paraná basin. UFRJ 7030, 18 ex., 28.1–60.7 mm SL; CICCAA 05603, 10 ex., 28.5–56.3 mm SL; all collected with holotype. – UFRJ 7031, 3 ex. (C&S), 36.7–57.7 mm SL; about 1.7 km below the type locality, 19°40'02"S, 47°01'34"W, about 940 m asl; W.M.S. Sampaio et al., 5 August 2021. – MZUSP 114937, 9 ex., 19.6–64.0 mm SL; stream tributary to Rio Quebra Anzol, 19°36'27"S, 46°54'57"W, about 983 m asl; O.T. Oyakawa et al., 26 June 2013. – MZUSP 114925, 15 ex., 14.4–55.2 mm SL; stream tributary to Rio Quebra Anzol at Araxá City, 19°35'37"S, 46°52'57"W, about 963 m asl; O.T. Oyakawa et al., 25 June 2013. – MZUSP 114918, 13 ex., 16.4–52.4 mm SL; stream tributary to Rio Quebra Anzol near Santuário Nossa Senhora de Fátima, 19°35'56"S, 46°54'51"W, about 1020 m asl; O.T. Oyakawa et al., 26 June 2013.

Additional specimens (non-types). MZUSP 109239, 2 ex.; Domo de Salitre; L.F. Salvador & M.J. Pozza, no date.

Diagnosis. *Trichomycterus araxa* is distinguished from all other species of the subgenus *Cryptocambeva* by the presence of a black median longitudinal stripe on the caudal fin in juvenile specimens below about 40 mm SL (Fig. 6; vs. black median longitudinal stripe always absent). *Trichomycterus araxa* differs from all other species of *Cryptocambeva*, except *T. macrotrichopterus*, by having a long pectoral-fin filament, its length about 40–60% of pectoral-fin length in specimens about 50 mm SL or larger (vs. short, about



Figure 4. *Trichomycterus araxa* sp. nov., holotype, UFRJ 7029, 53.6 mm SL **A.** Left lateral view; **B.** Dorsal view; **C.** Ventral view.

5–20%). *Trichomycterus araxa* is also distinguished from *T. macrotrichopterus* by the presence of the anterior infraorbital canal, supported by an elliptical antorbital (Fig. 8A; vs. anterior infraorbital canal absent, antorbital circular, Fig. 8D), a moderately deep opercular odontode patch (Fig. 8B; vs. slender, Fig. 8E), posterior margin of the metapterygoid, anterior margin of the hyomandibula anterior outgrowth and dorso-posterior margin of the quadrate slightly curved (Fig. 8B; vs. strongly waved, Fig. 8E), and absence of a prominent projection on the lateral margin of the lateral ethmoid, ventrally overlapping the sesamoid supraorbital (Fig. 8A; vs. presence, Fig. 8C).

Description. General morphology (Figs 4–7). Morphometric data appear in Table 1. Body moderately slender, subcylindrical, slightly depressed anteriorly, compressed posteriorly. Greatest body depth at vertical immediately anterior to pelvic-fin base. Dorsal and ventral profiles of head and trunk slightly convex, about straight on caudal peduncle. Anus and urogenital papilla at vertical just anterior to middle of dorsal-fin base. Head sub-trapezoidal in dorsal view. Anterior profile of snout slightly convex in dorsal view. Eye small, dorsally positioned in head, about equidistant from mouth and posterior border of opercle. Posterior nostril nearer anterior nostril than orbit. Tip of nasal barbel posteriorly reaching opercle or area slightly



Figure 5. Live holotype of *Trichomycterus araxa* sp. nov., UFRJ 7029, 53.6 mm SL, left lateral view.

Table 1. Morphometric data of *Trichomycterus araxa* sp. nov.

	Holotype	Paratypes (n = 10)	Mean
Standard length (mm)	53.6	43.3–64.0	53.5
Percent of standard length			
Body depth	19.3	15.8–20.9	18.5
Caudal peduncle depth	14.7	13.4–15.8	14.7
Body width	11.7	10.4–13.2	12.3
Caudal peduncle width	4.1	3.8–5.6	4.6
Pre-dorsal length	64.2	63.2–67.5	65.3
Pre-pelvic length	59.6	58.0–62.3	60.0
Dorsal-fin base length	11.6	11.4–14.2	12.4
Anal-fin base length	8.7	9.0–11.6	9.8
Caudal-fin length	19.0	17.3–20.2	18.9
Pectoral-fin length	15.0	12.3–14.6	13.3
Pelvic-fin length	10.2	9.7–11.3	10.5
Head length	20.2	19.4–21.6	20.1
Percent of head length			
Head depth	54.9	51.0–67.9	56.2
Head width	83.4	82.8–95.7	87.7
Snout length	47.2	42.4–48.7	45.9
Interorbital length	30.2	25.4–33.5	29.4
Preorbital length	11.6	9.4–13.6	11.5
Eye diameter	11.1	9.2–11.1	10.2

posterior to it; tip of maxillary barbel posteriorly reaching pectoral-fin base; rictal barbel posteriorly reaching area between interopercular patch of odontodes and pectoral-fin base. Mouth subterminal. Jaw teeth irregularly arranged, pointed, 35–49 in premaxilla, 32–45 in dentary. Head and trunk skin with minute skin papillae.

Dorsal and anal fins subtriangular, distal margin slightly convex; total dorsal-fin rays 10 or 11 (i–ii + II + 7), total anal-fin rays 9 (ii + II + 5); anal-fin origin at vertical through base of 5th branched dorsal-fin ray. Pectoral fin subtriangular in dorsal view, posterior margin slightly convex, first pectoral-fin ray terminating in long filament, reaching about 40–60% of pectoral-fin length in specimens above about 50 mm SL; total pectoral-fin rays 7 (I + 6). Pelvic fin subtruncate, its posterior extremity at vertical through middle of dorsal-fin base and posterior to urogenital aperture; pelvic-fin bases medially in contact; total pelvic-fin rays 5 (I + 4). Caudal

fin subtruncate, posterior corners rounded; total principal caudal-fin rays 13 (I + 11 + I), total dorsal procurent rays 20–23 (xix–xxii + I), total ventral procurent rays 16 or 17 (xv–xvi + I).

Laterosensory system. Supraorbital sensory canal continuous, posteriorly connected to posterior section of infraorbital canal. Supraorbital pores 3, all paired: s1, adjacent to medial margin of anterior nostril; s3, adjacent and just posterior to medial margin of posterior nostril; s6, at transverse line through posterior half of orbit. Pores s6 nearer its symmetrical homologous pore than orbit. Infraorbital sensory canal arranged in 2 segments; anterior section isolated, with two pores: i1, at transverse line through anterior nostril, i3, at transverse line just anterior to posterior nostril; posterior segment posteriorly connected to postorbital canal, with 2 pores: i10, adjacent to ventral margin of orbit, i11, posterior to orbit. Postorbital canal with 2 pores: po1, at vertical line above posterior portion of interopercular patch of odontodes, po2, at vertical line above posterior portion of opercular patch of odontodes. Lateral line of body short, with 1 pore just posterior to head.

Osteology (Fig. 8A–C). Mesethmoid T-shaped in dorsal view, cornu extremity rounded. Antorbital elliptical, short, dorso-posteriorly carrying thin latero-sensory canal. Sesamoid supraorbital slender, without processes. Premaxilla sub-rectangular in dorsal view, slightly narrowing laterally. Maxilla boomerang-shaped, shorter than premaxilla. Autopalatine sub-rectangular in dorsal view when excluding its postero-lateral process, its width about half its length including anterior cartilage; medial margin slightly sinuous, lateral margin about straight; posterolateral process well-developed, subtriangular, its length slightly shorter than autopalatine length excluding anterior cartilage. Lateral ethmoid with minute lateral projection. Metapterygoid sub-triangular, slightly longer than deep. Quadrate L-shaped, vertical branch wider, dorsoposterior margin in close proximity to hyomandibula outgrowth.

Hyomandibula long, with well-developed anterior outgrowth; middle portion of dorsal margin of hyomandibula slightly concave. Opercle slender, with moderately



Figure 6. *Trichomycterus araxa* sp. nov., paratype, UFRJ 7030, 26.4 mm SL: **A.** Left lateral view; **B.** Dorsal view; **C.** Ventral view.

deep odontode patch with 12–16 odontodes transversely arranged. Opercular odontodes pointed, anterior odontodes narrow and straight, posterior odontodes slightly broader, slightly curved. Dorsal process of opercle short. Opercular articular facet for hyomandibula with prominent rounded extension, articular facet for preopercle well developed, rounded. Interopercular patch of odontodes long, about four fifths of hyomandibula length, with 26–31 odontodes. Interopercular odontodes pointed, arranged in irregular longitudinal rows. Preopercle slender, narrowing anteriorly.

Parurohyal robust, lateral process subtriangular, latero-posteriorly directed, tip pointed; parurohyal head well-developed, with prominent anterolateral paired process; middle foramen oval circular; posterior process long, slightly shorter or equal to distance between anterior margin of parurohyal and anterior insertion of posterior process. Branchiostegal rays 8. Vertebrae 35. Ribs 12 or 13. Dorsal-fin origin at vertical through centrum of 19th vertebra; anal-fin origin at vertical through centrum of 22nd or 23rd vertebra. Two dorsal hypural plates, corresponding to hypurals 4 + 5 and 3, respectively; single

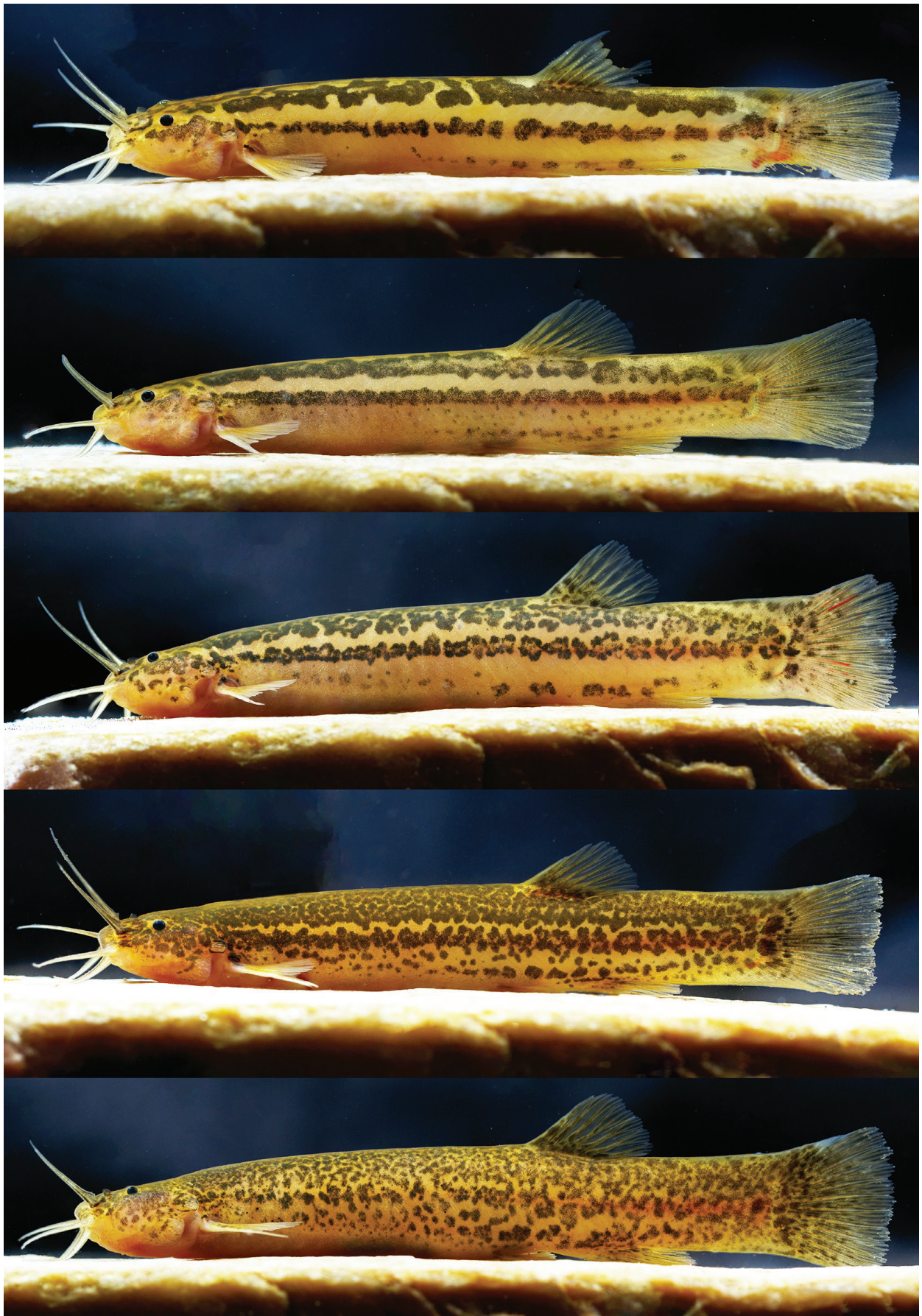


Figure 7. Live paratypes of *Trichomycterus araxa* sp. nov., UFRJ 7030, left lateral view: **A.** 40.6 mm SL; **B.** 39.3 mm SL; **C.** 53.7 mm SL; **D.** 45.8 mm SL; **E.** 45.8 mm SL.

ventral hypural plate corresponding to hypurals 1 and 2, and parhypural.

Colouration (Figs 4–7). Colouration of preserved specimens in alcohol similar to colouration in live specimens, except for yellow colouration being paler after preservation. Flank, dorsum and head side pale yellow, with variably shaped dark brown to black marks in adults. Smaller specimens (14.4–21.8 mm SL) with unspotted colouration and black narrow stripe along flank longitudinal midline. In specimens above about 25 mm SL, dark marks variably arranged and shaped, gradually changing in larger specimens, becoming more spotted and longitudinal midline stripe becoming fragmented or disappearing. Some specimens with dark marks arranged in three longitudinal zones (Fig. 7A–C), often forming large, coalesced blotches along dorsal region. In other specimens, longitudinal zones little or not distinct (Figs 4, 5, 7D, E), with spots being smaller and more scattered on flank in some specimens (Fig. 7E). Venter always white to yellowish white, paired fins hyaline. In smaller juveniles, about 14–40 mm SL (Fig. 6), fins hyaline, caudal fin with broad median black stripe anteriorly joined to flank midline stripe; in larger specimens,

unpaired fins gradually becoming faintly spotted on their bases, and caudal black stripe becoming inconspicuous in larger specimens (Figs 4, 5, 7).

Etymology. The name *araxa* is a reference to the occurrence of the new species in the region of Araxá, a historical Brazilian city founded in the 18th century, during the colonial period. The word *araxa* is possibly derived from the Tupi-Guarani to designate some native people formerly inhabiting the region.

Distribution and habitat notes. *Trichomycterus araxa* occurs in the Rio Quebra Anzol drainage, which is part of the Rio Paranaíba drainage, a main tributary of the upper Rio Paraná basin, in altitudes about 940–1020 m asl (Fig. 2). In the type locality area, the new species was collected in shallow, moderate fast-flowing streams, about 40–50 cm deep, and about 3–5 m wide, with a well-preserved marginal vegetation. The stream bottom comprised gravel, sand and pebbles. The new species was collected buried in the stream bank, but smaller specimens were sporadically seen swimming above gravel substratum. See Costa et al. (2022a) for a list of species occurring in this area, where this species is identified as *Trichomycterus* sp.

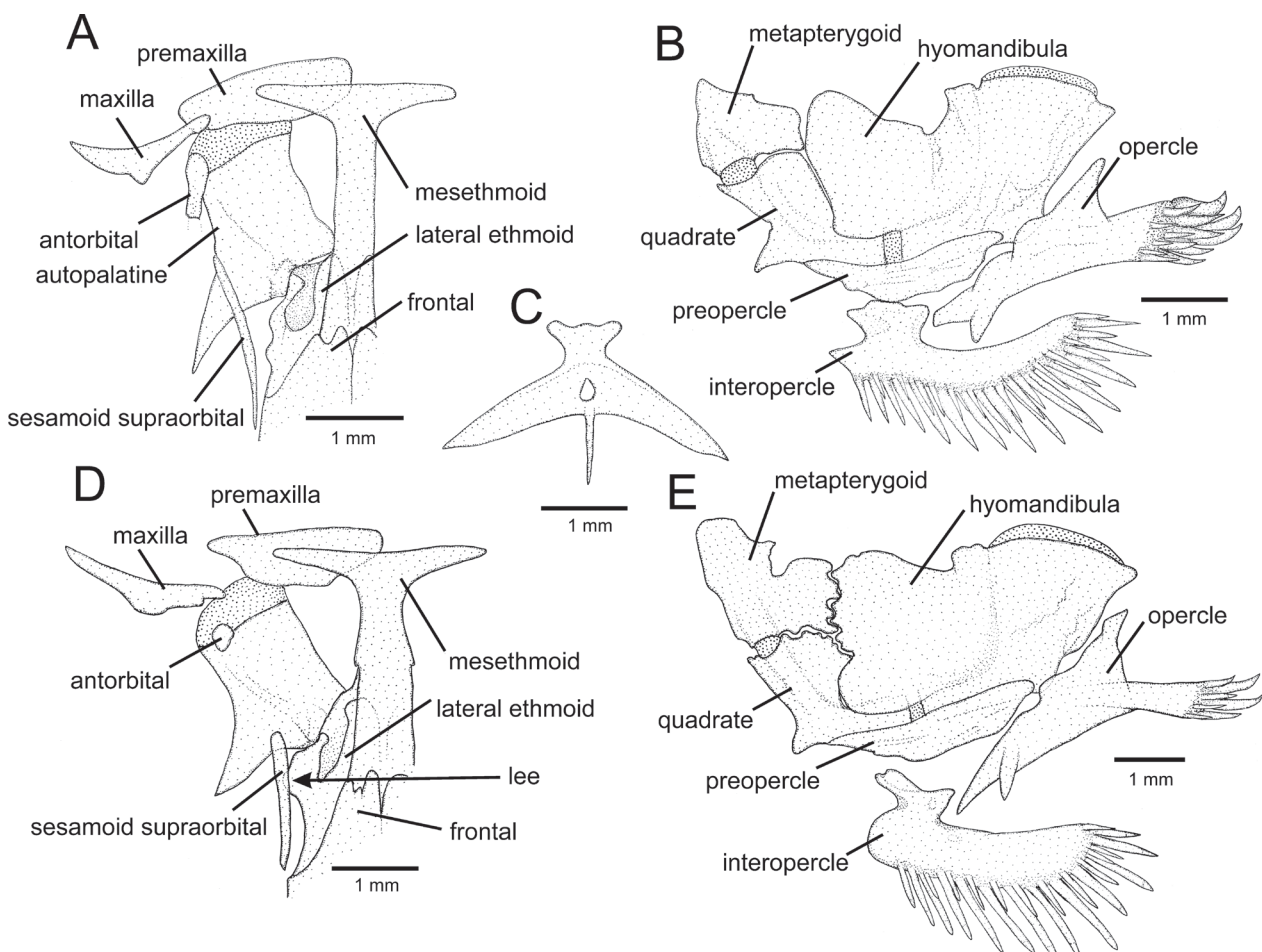


Figure 8. Osteological features in *Trichomycterus araxa* sp. nov. (A–C) and *T. macrotrichopterus* (D, E). A, D. Mesethmoidal region, middle and left portions, dorsal view; B, E. Left jaw suspensorium and opercular apparatus, lateral view; C. Parurohyal, ventral view. lee, lateral ethmoid expansion. Larger stippling represents cartilages.

Discussion

Phylogenetic relationships

Cryptocambeva occurs in a broad area of eastern South America, comprising different river basins and mountain ranges of south-eastern Brazil (Fig. 2; Costa 2021). *Trichomycterus araxa* is the second species of *Cryptocambeva* described from the Rio Paranaíba drainage. The first one was *Trichomycterus giarettai* Barbosa & Katz, 2016, occurring in another area of the drainage, at lower elevation, about 590 m asl (Barbosa and Katz 2016). Material of this species was not available for the present molecular phylogenetic analysis, but morphological data suggest that *T. giarettai* is closely related to *Trichomycterus candidus* (Miranda Ribeiro, 1949), not to *T. araxa*. *Trichomycterus giarettai* shares with *T. candidus* a thin premaxilla with few teeth (23–30), a condition that does not occur in *T. araxa* (i.e. 51–58 teeth) and in other species of *Cryptocambeva* and closely related subgenera, besides *T. giarettai* and *T. candidus* sharing a similar colour pattern, consisting of minute dark brown to black dots over a pale brownish yellow ground (Barbosa and Costa 2003: fig. 1; Barbosa and Katz 2016: fig. 1).

The phylogenetic analyses highly supported *T. araxa* as sister to *T. macrotrichopterus* (Fig. 1). However, the only morphological character state found to corroborate this sister group relationship was the presence of a long pectoral-fin filament, a condition not occurring in other species of *Cryptocambeva*, but sporadically occurring in other subgenera of *Trichomycterus* from eastern South America (Costa 1992). On the other hand, *T. araxa* does not exhibit any of the unique osteological features that are present in *T. macrotrichopterus*, including a prominent projection on the lateral margin of the lateral ethmoid (Fig. 8C), a strongly waved margin of the posterior margin of metapterygoid, anterior margin of hyomandibula anterior outgrowth and dorso-posterior margin of quadrate (Fig. 8D), and a distinctively slender opercular odontode patch (Fig. 8D), three conditions that do not occur in any other congener of the subgenus *Cryptocambeva*. In addition, it is remarkable that these species were found in different habitats, with *T. araxa* occurring in moderate fast-flowing streams with predominantly gravel bottom, and *T. macrotrichopterus* found in a fast-flowing river with large rocks on the bottom, just below waterfalls.

Timing of species diversification and biogeographical implications

Recent studies have shown a high concentration of closely related trichomycterine species in different South American regions, often exhibiting geographical distribution patterns restricted to some neighbouring river drainages around mountain and high plateau areas (e.g. Hayes et al. 2020; Costa et al. 2021c). However, the factors responsible for such distribution patterns and the high concentration of species in these areas have not been investigated. Herein we

tentatively associate the great species diversity of mountain trichomycterine catfishes concentrated between the headwaters of the Paraná and São Francisco basins with Cenozoic paleogeographic episodes that resulted in the present hydrographic configuration. The estimated age for the start of species diversification in *Cryptocambeva*, at the Middle Miocene, is chronologically compatible with the generalised uplift relief of south-eastern Brazil at this period as proposed by recent geological studies (Valadão 2009; Rezende et al. 2018). After an initial divergence during the Late Miocene, at about 8 Ma, separating *T. mimonha* lineage from another lineage comprising the most recent common ancestor of a clade containing all other species of *Cryptocambeva*, four main clades had their origins almost synchronically at about 6 Ma, still during the Late Miocene (Fig. 3). These clades are geographically disjunct, each one involving different mountain ranges and river basins (Figs 1, 2).

The divergence timing between *T. araxa* from the upper Rio Araguari and its sister group, *T. macrotrichopterus*, from the upper section of the main canal of the Rio São Francisco, at the Pliocene (Fig. 3), is also compatible with the period of intense fluvial re-arrangement reported for the region (Rezende et al. 2018). The upper Paranaíba uplift separating the Paraná and São Francisco river basins occurred in an older period, still in the Cretaceous (Campos and Dardenne 1997), but events of river segment captures changing river basin configuration in the upper Rio Paraná basin were frequent between the Middle Miocene and Pliocene (Rezende et al. 2018). Therefore, the divergence between *T. araxa* and *T. macrotrichopterus* estimated to have occurred at the Pliocene, is possibly derived from a drainage capture of the upper São Francisco by the upper Paranaíba drainage in the northeastern facet of the Serra da Canastra. This was a common paleogeographic event occurring in the region, well documented for the Rio Grande drainage, which captured a river drainage from the upper São Francisco basin (Rezende et al. 2018). However, this hypothesis should be still tested through the phylogenetic study of other fish groups inhabiting the same areas.

Acknowledgements

We are grateful to Valter M. Azevedo-Santos, for discussion about fish distribution patterns in the upper Paraná basin and help during type material collection. The manuscript benefitted from reviews provided by Francisco Langeani and Paulo Brito. Thanks are also due to the Meio Ambiente team of the Companhia Brasileira de Metalurgia e Mineração, for allowing collections and use of specimens from the farms comprising the RPPN São Sebastião and Monte Alto, and to Aléssio Datovo and Michel Gianeti by the loan of specimens. This work was partly supported by Conselho Nacional de Desenvolvimento Científico e Tecnológico (CNPq; grant 304755/2020-6 to WJEMC), Fundação Carlos Chagas Filho de Amparo à Pesquisa do Estado do Rio de Janeiro (FAPERJ; grant E-26/201.213/2021 to WJEMC, E-26/202.005/2020 to AMK, and E-26/202.327/2018 to JLM). This study was also supported by CAPES

(Coordenação de Aperfeiçoamento de Pessoal de Nível Superior, Finance Code 001) through Programa de Pós-Graduação em: Biodiversidade e Biologia Evolutiva/UFRJ; Genética/UFRJ; and Zoologia, Museu Nacional/UFRJ.

References

- Alencar AR, Costa WJEM (2006) *Trichomycterus pauciradiatus*, a new catfish species from the upper rio Paraná basin, southeastern Brazil (Siluriformes: Trichomycteridae). *Zootaxa* 1269(1): 43–49. <https://doi.org/10.11646/zootaxa.1269.1.3>
- Anisimova M, Gil M, Dufayard JF, Dessimoz C, Gascuel O (2011) Survey of branch support methods demonstrates accuracy, power, and robustness of fast likelihood-based approximation schemes. *Systematic Biology* 60(5): 685–699. <https://doi.org/10.1093/sysbio/syr041>
- Arratia G, Huaquin L (1995) Morphology of the lateral line system and of the skin of diplomystid and certain primitive loricarioid catfishes and systematic and ecological considerations. *Bonner Zoologische Monographien* 36: 1–110.
- Barbosa MA, Costa WJEM (2003) Validade, relações filogenéticas e redescoberta de *Eremophilus candidus* Ribeiro, 1949 (Teleostei, Siluriformes, Trichomycteridae). *Arquivos do Museu Nacional, Museu Nacional (Brazil)* 61: 179–188.
- Barbosa MA, Costa WJEM (2010) Seven new species of the catfish genus *Trichomycterus* (Teleostei: Siluriformes: Trichomycteridae) from Southeastern Brazil and redescription of *T. brasiliensis*. *Ichthyological Exploration of Freshwaters* 21: 97–122.
- Barbosa MA, Katz AM (2016) A new species of the catfish genus *Trichomycterus* (Teleostei: Siluriformes: Trichomycteridae) from the Paranaíba basin, Central Brazil. *Vertebrate Zoology* 66: 261–265.
- Betancur-R R, Ortí G, Pyron RA (2015) Fossil-based comparative analyses reveal ancient marine ancestry erased by extinction in ray-finned fishes. *Ecology Letters* 18(5): 441–450. <https://doi.org/10.1111/ele.12423>
- Bockmann FA, Sazima I (2004) *Trichomycterus maracaya*, a new catfish from the upper rio Paraná, southeastern Brazil (Siluriformes: Trichomycteridae), with notes on the *T. brasiliensis* species-complex. *Neotropical Ichthyology* 2(2): 61–74. <https://doi.org/10.1590/S1679-62252004000200003>
- Campos JEG, Dardenne MA (1997) Origem e evolução da Bacia São-franciscana. *Revista Brasileira de Geociências* 27(3): 283–294. <https://doi.org/10.25249/0375-7536.1997283294>
- Chenna R, Sugawara H, Koike T, Lopez R, Gibson TJ, Higgins DG, Thompson JD (2003) Multiple sequence alignment with the Clustal series of programs. *Nucleic Acids Research* 31(13): 3497–3500. <https://doi.org/10.1093/nar/gkg500>
- Chernomor O, von Haeseler A, Minh BQ (2016) Terrace aware data structure for phylogenomic inference from supermatrices. *Systematic Biology* 65(6): 997–1008. <https://doi.org/10.1093/sysbio/syw037>
- Close B, Banister K, Baumans V, Bernoth EM, Bromage N, Bunyan J, Erhardt W, Flecknell P, Gregory N, Hackbarth H, Morton D, Warwick C (1996) Recommendations for euthanasia of experimental animals: Part 1. *Laboratory Animals* 30(4): 293–316. <https://doi.org/10.1258/002367796780739871>
- Close B, Banister K, Baumans V, Bernoth EM, Bromage N, Bunyan J, Erhardt W, Flecknell P, Gregory N, Hackbarth H, Morton D, Warwick C (1997) Recommendations for euthanasia of experimental animals: Part 2. *Laboratory Animals* 31(1): 1–32. <https://doi.org/10.1258/002367797780600297>
- Costa WJEM (1992) Description de huit nouvelles espèces du genre *Trichomycterus* (Siluriformes: Trichomycteridae), du Brésil oriental. *Revue Française d'Aquariologie et Herpetologie* 18: 101–110.
- Costa WJEM (2021) Comparative osteology, phylogeny and classification of the eastern South American catfish genus *Trichomycterus* (Siluriformes: Trichomycteridae). *Taxonomy* 1(2): 160–191. <https://doi.org/10.3390/taxonomy1020013>
- Costa WJEM, Katz AM (2021) Integrative taxonomy supports high species diversity of south-eastern Brazilian mountain catfishes of the *T. reinhardti* group (Siluriformes: Trichomycteridae). *Systematics and Biodiversity* 19(6): 601–621. <https://doi.org/10.1080/14772000.2021.1900947>
- Costa WJEM, Katz AM, Mattos JLO, Amorim PF, Mesquita BO, Vilarado PJ, Barbosa MA (2020a) Historical review and redescription of three poorly known species of the catfish genus *Trichomycterus* from south-eastern Brazil (Siluriformes: Trichomycteridae). *Journal of Natural History* 53(47–48): 2905–2928. <https://doi.org/10.1080/00222933.2020.1752406>
- Costa WJEM, Henschel E, Katz AM (2020b) Multigene phylogeny reveals convergent evolution in small interstitial catfishes from the Amazon and Atlantic forests (Siluriformes: Trichomycteridae). *Zoologica Scripta* 49(2): 159–173. <https://doi.org/10.1111/zsc.12403>
- Costa WJEM, Mattos JLO, Katz AM (2021a) Two new catfish species from central Brazil comprising a new clade supported by molecular phylogeny and comparative osteology (Siluriformes: Trichomycteridae). *Zoologischer Anzeiger* 293: 124–137. <https://doi.org/10.1016/j.jcz.2021.05.008>
- Costa WJEM, Mattos JLO, Katz AM (2021b) Phylogenetic position of *Trichomycterus payaya* and examination of osteological characters diagnosing the Neotropical catfish genus *Ituglanis* (Siluriformes: Trichomycteridae). *Zoological Studies (Taipei, Taiwan)* 60: e43. <https://doi.org/10.6620/ZS.2021.60-43>
- Costa WJEM, Feltrin CRM, Katz AM (2021c) Field inventory reveals high diversity of new species of mountain catfishes, genus *Cambeva* (Siluriformes: Trichomycteridae), in south-eastern Serra Geral, southern Brazil. *Zoosystema* 43: 659–690. <https://doi.org/10.5252/zoosystema2021v43a28>
- Costa WJEM, Sampaio WMS, Giongo P, de Almeida FB, Azevedo-Santos VM, Katz AM (2022a) An enigmatic interstitial trichomycterine catfish from south-eastern Brazil found at about 1000 km away from its sister group (Siluriformes: Trichomycteridae). *Zoologischer Anzeiger* 297: 85–96. <https://doi.org/10.1016/j.jcz.2022.02.007>
- Costa WJEM, Mattos JLO, Lopes S, Amorim PF, Katz AM (2022b) Integrative taxonomy, distribution and ontogenetic colouration change in Neotropical mountain catfishes of the *Trichomycterus nigroauratus* group (Siluriformes: Trichomycteridae). *Zoological Studies (Taipei, Taiwan)* 61: e11.
- Cramer CA, Bonatto SL, Reis RE (2011) Molecular phylogeny of the Neoplecostominae and Hypoptopomatinae (Siluriformes: Loricariidae) using multiple genes. *Molecular Phylogenetics and Evolution* 59(1): 43–52. <https://doi.org/10.1016/j.ympev.2011.01.002>
- Gernhard T (2008) The conditioned reconstruction process. *Journal of Theoretical Biology* 253(4): 769–778. <https://doi.org/10.1016/j.jtbi.2008.04.005>
- Guindon S, Dufayard JF, Lefor V, Anisimova M, Hordijk W, Gascuel O (2010) New algorithms and methods to estimate maximum-likelihood

- phylogenies: Assessing the performance of PhyML 3.0. *Systematic Biology* 59(3): 307–321. <https://doi.org/10.1093/sysbio/syq010>
- Hayes MM, Paz HJ, Stout CC, Werneke DC, Armbruster JW (2020) A hotspot atop: rivers of the Guyana Highlands hold high diversity of endemic pencil catfish (Teleostei: Ostariophysi: Siluriformes). *Biological Journal of the Linnean Society*. Linnean Society of London 129(4): 862–874. <https://doi.org/10.1093/biolinnean/blaa023>
- Hoang DT, Chernomor O, von Haeseler A, Minh BQ, Vinh LS (2018) UFBoot2: Improving the ultrafast bootstrap approximation. *Molecular Biology and Evolution* 35(2): 518–522. <https://doi.org/10.1093/molbev/msx281>
- Kalyaanamoorthy S, Minh BQ, Wong TKF, von Haeseler A, Jermini LS (2017) ModelFinder: Fast model selection for accurate phylogenetic estimates. *Nature Methods* 14(6): 587–589. <https://doi.org/10.1038/nmeth.4285>
- Katz AM, Barbosa MA, Mattos JLO, Costa WJEM (2018) Multigene analysis of the catfish genus *Trichomycterus* and description of a new South American trichomycterine genus (Siluriformes, Trichomycteridae). *Zoosystematics and Evolution* 94(2): 557–566. <https://doi.org/10.3897/zse.94.29872>
- Kumar S, Stecher G, Li M, Knyaz C, Tamura K (2018) MEGAX: Molecular Evolutionary Genetics Analysis across computing platforms. *Molecular Biology and Evolution* 35(6): 1547–1549. <https://doi.org/10.1093/molbev/msy096>
- Lanfear R, Frandsen PB, Wright AM, Senfeld T, Calcott B (2016) PartitionFinder 2: New methods for selecting partitioned models of evolution for molecular and morphological phylogenetic analyses. *Molecular Biology and Evolution* 34: 772–773. <https://doi.org/10.1093/molbev/msw260>
- Leary S, Underwood W, Anthony R, Cartner S, Corey D, Grandin T (2013) AVMA guidelines for the euthanasia of animals. http://works.bepress.com/cheryl_greenacre/14
- Minh BQ, Nguyen MAT, von Haeseler A (2013) Ultrafast approximation for phylogenetic bootstrap. *Molecular Biology and Evolution* 30(5): 1188–1195. <https://doi.org/10.1093/molbev/mst024>
- Nguyen LT, Schmidt HA, von Haeseler A, Minh BQ (2015) IQ-TREE: A fast and effective stochastic algorithm for estimating maximum likelihood phylogenies. *Molecular Biology and Evolution* 32(1): 268–274. <https://doi.org/10.1093/molbev/msu300>
- Oliveira OS, Marquis RJ (2002) Introduction: development of research in the Cerrados. In: Oliveira PS, Marquis RJ (Eds) *The Cerrados of Brazil, ecology and natural history of a Neotropical savanna*. Columbia University Press, New York, 1–10. <https://doi.org/10.7312/oliv12042-intro>
- Palumbi S, Martin A, Romano WO, Stice L, Grabowski G (1991) The simple fool's guide of PCR, version 2.0. University of Hawaii, Honolulu.
- Rambaut A, Drummond AJ, Xie D, Baele G, Suchard MA, Rambaut A, Drummond AJ, Xie D, Baele G, Suchard MA (2018) Posterior summarisation in Bayesian phylogenetics using Tracer 1.7. *Systematic Biology* 67(5): 901–904. <https://doi.org/10.1093/sysbio/syy032>
- Rezende EA, Salgado AAR, Castro PTA (2018) Evolução da rede de drenagem e evidências de antigas conexões entre as bacias dos rios Grande e São Francisco no sudeste brasileiro. *Revista Brasileira de Geomorfologia* 19(3): 483–501. <https://doi.org/10.20502/rbg.v19i3.1304>
- Riccomini C, Sant'anna LG, Ferrari AL (2004) Evolução geológica do Rift Continental do Sudeste do Brasil. In: Mantesso-Neto V, Bartorelli A, Carneiro CDR, Brito-Neves BB (Eds) *Geologia do continente Sul-Americano: evolução da obra de Fernando Flávio Marques de Almeida*. Beca, São Paulo, 383–405.
- Ronquist F, Teslenko M, Van der Mark P, Ayres DL, Darling A, Höhna S, Larget B, Liu L, Suchard MA, Huelsenbeck JP (2012) MrBayes 3.2: Efficient Bayesian phylogenetic inference and model choice across a large model space. *Systematic Biology* 61(3): 539–542. <https://doi.org/10.1093/sysbio/sys029>
- Schwarz G (1978) Estimating the dimension of a model. *Annals of Statistics* 6(2): 461–464. <https://doi.org/10.1214/aos/1176344136>
- Suchard MA, Lemey P, Baele G, Ayres DL, Drummond AJ, Rambaut A (2018) Bayesian phylogenetic and phylodynamic data integration using BEAST 1.10. *Virus Evolution* 4(1): vey016. <https://doi.org/10.1093/ve/vey016>
- Sullivan JP, Lundberg JG, Hardman M (2006) A phylogenetic analysis of the major groups of catfishes (Teleostei: Siluriformes) using rag1 and rag2 nuclear gene sequences. *Molecular Phylogenetics and Evolution* 41(3): 636–662. <https://doi.org/10.1016/j.ympev.2006.05.044>
- Taylor WR, Van Dyke GC (1985) Revised procedures for staining and clearing small fishes and other vertebrates for bone and cartilage study. *Cybiurn* 9: 107–119.
- Trifinopoulos J, Nguyen L-T, von Haeseler A, Minh BQ (2016) IQ-TREE: A fast online phylogenetic tool for maximum likelihood analysis. *Nucleic Acids Research* 44(W1): W232–W235. <https://doi.org/10.1093/nar/gkw256>
- Triques ML, Vono V (2004) Three new species of *Trichomycterus* (Teleostei: Siluriformes: Trichomycteridae) from the Rio Jequitinhonha basin, Minas Gerais, Brazil. *Ichthyological Exploration of Freshwaters* 15: 161–172.
- Valadão RC (2009) Geodinâmica de Superfícies de Aplanamento, Desnudação Continental e Tectônica Ativa como condicionantes da Megageomorfologia do Brasil Oriental. *Revista Brasileira de Geomorfologia* 10(2): 77–90. <https://doi.org/10.20502/rbg.v10i2.132>
- Villa-Verde L, Lazzarotto H, Lima SQM (2012) A new glanapterygine catfish of the genus *Listrura* (Siluriformes: Trichomycteridae) from southeastern Brazil, corroborated by morphological and molecular data. *Neotropical Ichthyology* 10(3): 527–538. <https://doi.org/10.1590/S1679-62252012000300005>

Supplementary material 1

Tables S1, S2

Authors: Wilson J. E. M. Costa, José Leonardo O. Mattos, Wagner M. S. Sampaio, Patrícia Giongo, Frederico B. de Almeida, Axel M. Katz

Data type: pdf file

Explanation note: **Table S1**. Terminal taxa for molecular phylogeny and respective GenBank accession numbers. **Table S2**. Best-fitting models.

Copyright notice: This dataset is made available under the Open Database License (<http://opendatacommons.org/licenses/odbl/1.0/>). The Open Database License (ODbL) is a license agreement intended to allow users to freely share, modify, and use this Dataset while maintaining this same freedom for others, provided that the original source and author(s) are credited.

Link: <https://doi.org/10.3897/zse.98.83109.suppl1>